Energy Distribution in Keyhole Mode Plasma Arc Welds

A study of the parameters that produce the keyhole behavior in plasma arc welding promises improved process control

BY M. J. TOMSIC AND C. E. JACKSON

ABSTRACT. A phenomenon occurs during plasma arc welding which is not commonly found with any other welding process. During plasma arc welding, the base metal can be penetrated completely and a hole formed at the point of welding that is carried along as the weld progresses. This phenomenon, called keyhole mode plasma arc welding, is used in a limited range of thickness, for example, 304 stainless steel 3/32 to 1/4 in. (2.4 to 6.0 mm) with conventional plasma arc welding torches. The broad objective of this program is to study the controlling parameters associated with the formation of the keyhole in plasma arc welds.

The results indicate that a fused area between the keyhole and the base metal is present after the arc is established and the torch is moving. The shape of the weld is the result of a balance among the plasma gas pressure, the surface tension that supports the molten metal and the backing gas pressure. When the keyhole is established and traveling along the weld, the molten metal flows around the sides of the arc and back along the weld behind the keyhole. When the molten metal leaves the region of the plasma arc pressure, the only forces remaining to support the molten metal are the surface tension and the backing gas pressure which is part of the process. If the heat input of the plasma arc weld is insufficient or the orifice gas flow is too low, the plasma arc will not penetrate the material. On the other hand, if the heat input or gas flow is excessive, the keyhole widens. Where this occurs, the enlarged mass of molten metal displaced by the keyhole flows back behind the keyhole for a longer distance and a uniform bead is not obtained. Data obtained from test welds indicate the mechanism for producing and the parameters for controlling keyhole weld behavior.

M. J. TOMSIC is with the Babcock & Wilcox Research Laboratories, Alliance, Ohio. C. E. JACKSON is Associate Professor, Department of Welding Engineering, the Ohio State University, Columbus, Ohio.

Paper was presented at the 54th AWS Annual Meeting held in Chicago during April 2-6, 1973.

Introduction

The progress of welding over the past few decades has been due largely to better understanding and control of the quantity and location of heat in the weld area. This progress has led to wider use of new welding processes such as electron beam, laser, and plasma arc welding, which are highly capable of controlling energy input into the weld. Plasma arc welding as a useful process is relatively new, being only about 20 years old (Refs. 1-13). The plasma arc welding process provides some distinct advantages such as excellent root contour, increased travel speeds, and lower heat input compared to competitive welding processes.

In most applications of plasma arc welding, the base metal is penetrated completely and a hole is formed at the point of welding that is carried along as the weld progresses. This phenomenon, called keyhole mode plasma arc welding (or keyholing), is used in a limited range of thickness, for example, type 304 stainless steel in 3/32 to 1/4 in. (2.4 to 6.0 mm). Several investigators have reported

their findings (Refs. 12,13) in studies of keyhole mode plasma arc welding and its applications.

To understand the "keyhole" phenomenon, the energy distribution in the arc and the transfer of arc energy to the base metal needs to be investigated. Since energy transferred to the base metal results in molten metal, the flow of the molten liquid should also be considered. A study of the effect of the variables of the plasma arc welding process should lead to a better understanding of the keyhole mode. The possibility of applications of keyhole mode plasma arc welding in new materials, new designs and to thicknesses beyond the present technology is suggested.

Objectives

The broad objective of this program was to study the phenomenon associated with the formation of a keyhole in high quality plasma arc welds. The specific objectives of this program which were studied included:

1. An examination of the relationship between the plasma arc welding parameters and the process and melting efficiencies of the keyhole mode plasma arc welds.
2. An examination of the relationship between the plasma arc welding parameters and the shape of the weld metal cross-section with specific attention to the top and bottom widths of keyhole type welds.
3. An examination of the relationship between the welding parameters, efficiencies, and dimensions of keyhole mode plasma arc welds for the purpose of determining the energy distribution for this type of weld.

Experimental Procedure and Apparatus

The material that was used for the welds in these experiments was type 304 stainless steel (18% Cr, 8% Ni) in a sheet thickness of 1/8 in. (3 mm).

Plasma arc welds, keyhole mode, were made using the following equipment:

1. Linde PWM-4 Needle Arc Welder
2. Linde PT-12 Plasma Needle Arc Torch, 100A capacity, connected for straight polarity, electrode negative (Fig. 1)
3. Linde C-200C constant current power supply
4. Linde type C electronic governor to drive the machine carriage
5. Two Esterline Angus Meters 50 mV-150 V multipurpose recorders for continuously recording current and voltage.

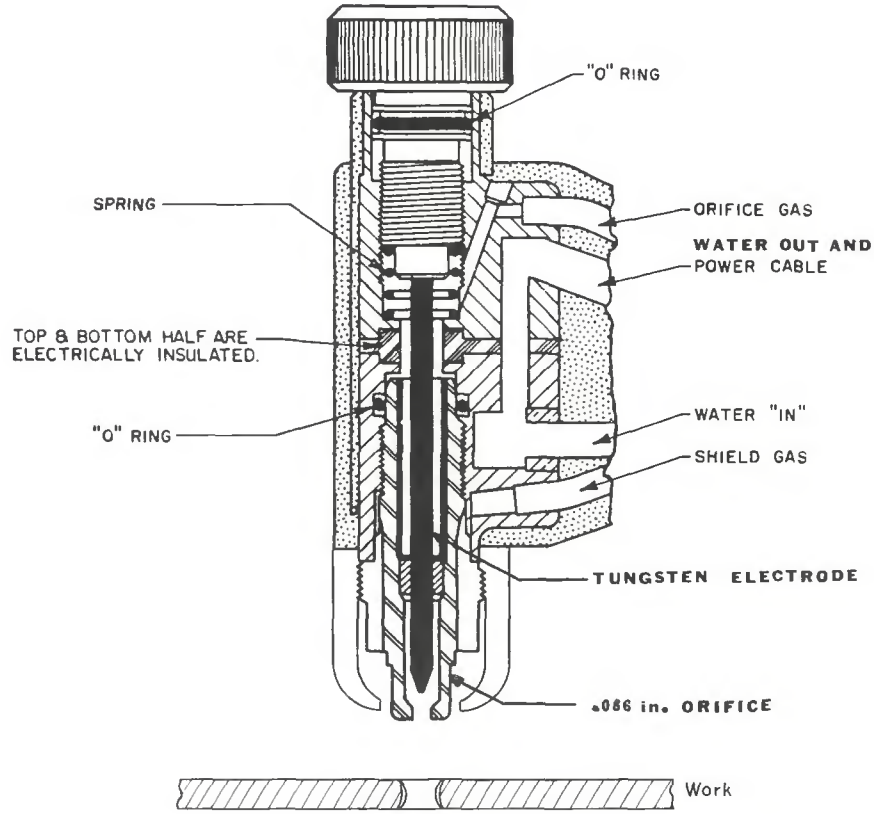

Fig. 1 — Cross section of the plasma needle arc torch. Dimension scale established by 1/8 in. (3 mm) work material thickness

The following parameters were not changed unless otherwise stated:

1. The orifice flow gas was argon
2. The shielding gas was argon at 30 cfh (236×10^3 mm^3/s)
4. A 3/32 in. (2.4 mm) tungsten, 1% thoriated electrode with a 45 deg included angle point was used
5. A water cooled 0.086 in. (2.2 mm) copper orifice and a No. 6 ceramic shielding cup was used
6. The pilot arc current was maintained at 7 A
7. The torch was kept normal to the weld surface
8. All welds were made welding away from the ground connection
9. All welds were made with the tungsten electrode connected to the negative terminal (dcsp)

To determine the effect of each welding parameter on a keyhole type weld, the four primary welding parameters, travel speed, current, orifice gas flow and arc length were varied one at a time.

Method of Calculating Process Efficiency

Many investigators have reported studies in which the energy input has been expressed as total arc energy per linear unit. This has been successful as a control measure in past years where limited current ranges and travel speeds were used. In many investigations the efficiency of heat utilization in melting and heating the plate has been considered to be a process constant. Other investigators have indicated that process efficiency changes with variations in welding parameters. The effect of changing welding parameters and arc characteristics have been considered in this investigation.

For determining process efficiency the heat conduction equation for a line heat source presented by Rosenthal (Ref. 14) was used. A chromel-alumel thermocouple was used to record the thermal cycle at a point some distance from the weld.

$$t - t_o = \frac{Q_p\, e^{-(\lambda v \xi)} K_o(\lambda vr)}{2\pi k g} \qquad (1)$$

The basic Rosenthal equation may be rearranged and solved for Q_p:

$$Q_p = \frac{(t - t_o) 2\pi k g}{e^{-(\lambda v \xi)} K_o(\lambda vr)} \qquad (2)$$

See Table 1 for symbol designation and units. The average temperature between room and the peak temperature of the thermocouple was used for determining the value of thermal conductivity, k, and thermal diffu-

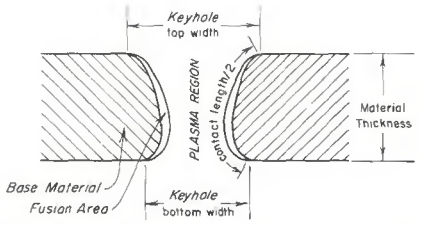

Fig. 2 — Measurement of keyhole top width, bottom width, and contact length. During welding the fusion area is liquid

sivity, λ (Refs. 15, 16). The process efficiency, Z_p, becomes:

$$Z_p = \left(\frac{Q_p}{VA}\right) 100 \quad (3)$$

Method of Calculating Melting Efficiency

Melting efficiency considers the energy used to melt the weld metal. The melting efficiency can be calculated using the electrical energy input, the cross-sectional area of the weld bead (nugget area), and the energy necessary to raise the weld metal from room temperature to the superheated temperature of the weld pool. The electrical energy input was measured during welding; the nugget area was determined from macrophotographs. The energy to raise the weld metal from room temperature to the superheated temperature of the weld pool was calculated using the following formula.

$$W = \left[\int_{t_o}^{tm} c_s \, dt + \Delta H + \int_{tm}^{t} c_l \, dt\right]\rho \quad (4)$$

With an initial temperature, t_0, of 20 C and assuming the weld pool is heated to 200 C above the melting temperature (Ref. 17), the energy per unit volume equals 9.5418 joules/mm³ (148.184 Btu/in³). The melting efficiency, Z_m, is given as follows:

$$Z_m = \left(\frac{W\,(na)}{VA/v}\right) 100 \quad (5)$$

Relationship Between Process Efficiency and Keyhold Dimensions

The energy across the plasma-liquid metal boundary is given by the equation:

$$q_s = \frac{Q_p}{vL} \quad (6)$$

The energy per unit area, q_s, was calculated for each of the weld samples for which the process efficiency was measured. This energy per unit area implies that a temperature gradient exists across the plasma-molten metal boundary. If it is assumed that the molten liquid is always at the same temperature, the energy per unit area gives an indication of the plasma boundary temperature. As the energy per unit area increases, the plasma boundary temperature increases, and as the energy per unit area decreases, the plasma boundary temperature decreases.

Table 1 — Symbols, Metric Units and U.S. Customary Equivalents

Symbols	Designation	Metric Units	Customary Units
x,y	Point coordinates	mm	= 0.03937 in.
v	Welding speed	mm/s	= 0.03937 in./s
t	Point temperature	C	= 5/9 (F−32)
t_0	Initial temperature	C	= 5/9 (F −32)
s	Time	second	= second
ξ	x - vs	mm	= 0.03937 in.
r	$(\xi^{2}+y^{2})^{1/2}$	mm	= 0.03937 in.
g	Plate thickness	mm	= 0.03937 in.
Q_p	Plate heat input	joule/s	= 9.480×10^{-4} Btu/s
λ	Thermal diffusivity	s/mm²	= 6.452×10^{2} s/in.²
k	Thermal conductivity	joule/mm-C-s	= 1.338×10^{-2} Btu/in.-F-s
V	Voltage	volt	= volt
A	Electrical current	ampere	= ampere
VA	Electrical power	joule/s	= watt
Z_p	Process efficiency	%	= %
W	Energy per unit volume	joule/mm³	= 15.53 Btu/in.³
t_m	Melting temperature[a]	C	= 5/9 (F −32)
c_s	Specific heat (solid)[a]	joule/g-C	= 0.239 Btu/lb-F
c_l	Specific heat (liquid)[b]	joule/g-C	= 0.239 Btu/lb-F
ΔH	Latent heat of fusion[b]	joule/g	= 0.430 Btu/lb
ρ	Density[a]	g/mm³	= 36.13 lb/in.³
Z_m	Melting efficiency	%	= %
na	Weld bead nugget area	mm²	= 0.00155 in.²
L	Contact length (Fig. 2)	mm	= 0.03937 in.
q_s	Energy per unit area	joule/mm²	= 0.6116 Btu/in.²
K_o	Bessel function of second kind and zero order		
e	Base of natural logarithms		

(a) For 304 stainless steel: melting temperature = 1410 C; specific heat (solid) = 0.6026 J/g-C (see Ref. 15); density = 7.585×10^{-3} g/mm³ (see Ref. 16).
(b) For iron: specific heat (liquid) = 0.7533 J/g-C (Ref. 15); latent heat of fusion = 272.03 J/g (Ref. 16).

Determination of Top Keyhole Width, Bottom Keyhole Width and Contact Length

To analyze the shape of the keyhole type weld, the weld samples were cross-sectioned, polished, and etched, across the width of the keyhole as shown in the sketch in Fig. 2. The top and bottom keyhole width and the contact length were recorded from photographs. The contact length, L, is the total length on both sides of the boundary between the fusion area and the plasma region.

Results and Discussion

As the arc is initiated, the weld surface melts, and the force of the plasma resulting from the plasma constriction allows some of the arc energy to be available for transfer deeper into the base metal. This penetration continues until the force of the plasma jet is consumed, or the base metal is penetrated completely by the arc. The hole that forms during and after welding is round, as shown in Fig. 3. There appears to be a minimum plasma jet force to enable the penetration of a certain type and thickness of base metal. It was assumed that the dynamic characteristics of extinguishing the arc did not affect significantly the shape of the keyhole.

A cross-section of a typical keyhole is shown in Fig. 4. The hole starts out wide at the top, narrows down, and at a distance just above the bottom of the plate, the hole starts increasing in width. In the cross-section, a fusion zone between the hole and the base metal can be seen. This is the molten metal that is present when the arc is established and the torch is moving. The arc plasma flow pattern is the same as the keyhole shape. At the bottom of the keyhole where the hole starts to enlarge, the fusion zone narrows down so that an interface between base metal, fusion zone and plasma, as shown in Fig. 2 is formed.

It appears that the plasma gas pressure and the surface tension support the molten metal on the sides of the keyhole while the arc is moving. When the keyhole is established and traveling along the weld, the molten metal flows around the sides of the plasma arc and back along the weld behind the keyhole. When the molten metal leaves the region of the plasma arc pressure, the only forces remaining to support the molten metal are surface tension and the backing gas pressure. One of the keyhole welds was sectioned in six places to show how the keyhole cross-section changes throughout the keyhole area. Figure 5 shows the location and

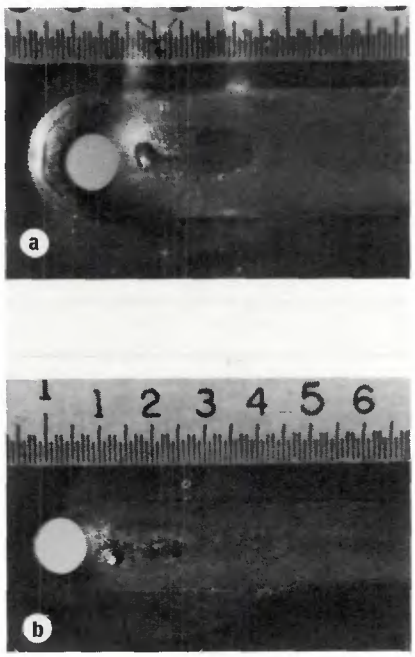

Fig. 3 — Keyhole mode plasma arc weld. (a) Top side, (b) Bottom side. The weld specimen was made at 85 A, 24 V, ¼ in. (6.3 mm) arc length, 6 cfh (39 × 10^3 mm^3/s) orifice flow, and 5.0 ipm (2.12 mm/s) travel speed

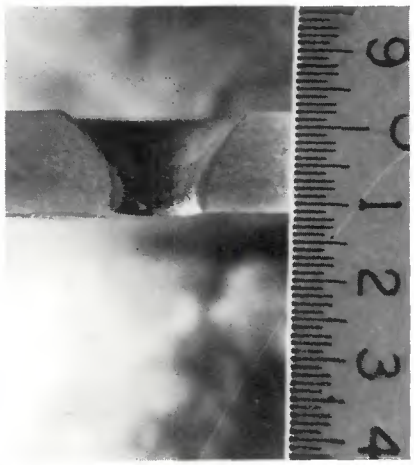

Fig. 4 — Cross section through center of a keyhole mode plasma arc weld. Welding parameters: 86 A, 22.5 V, ¼ in. (6.3 mm) arc length, 10 cfh (78.6 × 10^3 mm^3/s) orifice gas and 6.5 ipm (2.75 mm/s) travel speed

shape of these cross sections.

If the heat input of a plasma arc weld is insufficient or the orifice gas flow is too low, the plasma arc will not penetrate the work material. On the other hand, if the heat input or the gas flow is excessive, the keyhole widens. The mass of molten metal displaced by the keyhole keeps flowing back behind the keyhole for a longer distance and a uniform bead is not obtained. As shown in Fig. 6, the molten metal flows back and surface tension collects this molten metal into humps. When a hump solidifies a new one starts forming at the bottom of the base plate.

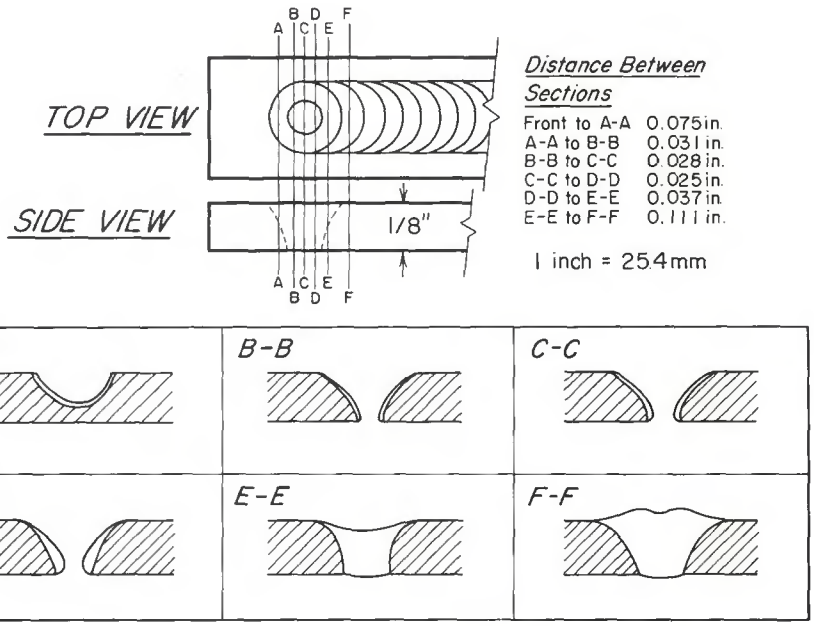

Fig. 5 — Sketches showing cross sections through a keyhole mode plasma arc weld

In some cases, undercutting can develop in keyhole plasma arc welds. If the undercut is on one side, the current probably is not evenly distributed to both sides of the keyhole, a condition which produces uneven magnetic fields. If the orifice gas flow is greater than necessary to penetrate the base material, an undercut may appear on both sides of the weld. Under this condition the molten metal sinks down in the weld, and does not wet into the top edges of the weld.

Both the process and melting efficiencies decrease as the current (heat input) increases. This decrease in efficiency shown in Fig. 7 is partially accounted for by the fact that as the current is increased, the keyhole width becomes larger so the percent of heat loss out the bottom of the keyhole increases, leaving less heating of the base metal. Niles (Ref. 18) also shows the same decrease of process efficiency with increased current level for the "melt-in-mode" gas tungsten-arc process. This effect of decreased process efficiency can partially be accounted for by (1) a larger loss of heat in the arc column and cathode regions of the arc, and (2) a larger heat loss at the bottom of the keyhole. The same trend of decreasing process and melting efficiency as the heat input increases is shown in Fig. 8 where the travel speed is varied. The process and melting efficiency increases as the travel speed increases; again, the same reasons as given above for the effect of current can be used to account for this increase.

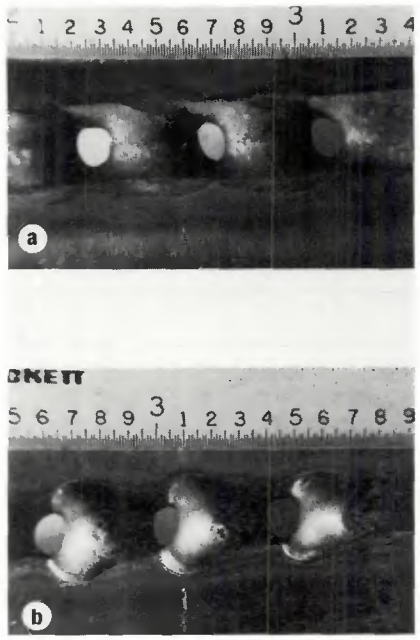

Fig. 6 — Humps that form on the bottom of the base metal of a keyhole mode plasma arc weld when the heat input is too high; (a) shows the top side and (b) shows the bottom side of the weld. Welding conditions: 121 A, 27 V, ¼ in. (6.3 mm) arc length, 6 cfh (39 × 10^3 mm^3/s) orifice gas flow and 6.5 ipm (2.75 mm/s) travel speed

The orifice gas flow was varied with constant heat input and arc length. Figure 9 shows the process and melting efficiency plotted for a range of orifice gas flows. As the orifice gas flow increases, the melting and process efficiency decreases. It is to be noted that with an orifice gas flow increase, the width of the bottom of the keyhole increases allowing

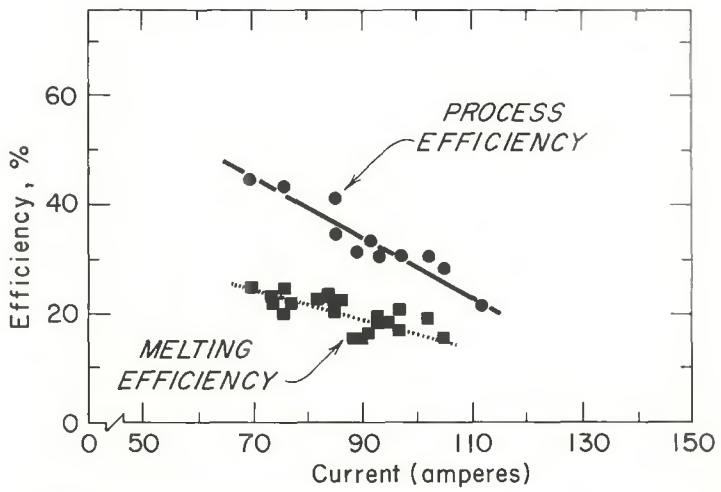

Fig. 7 — Effect of current on process and melting efficiency

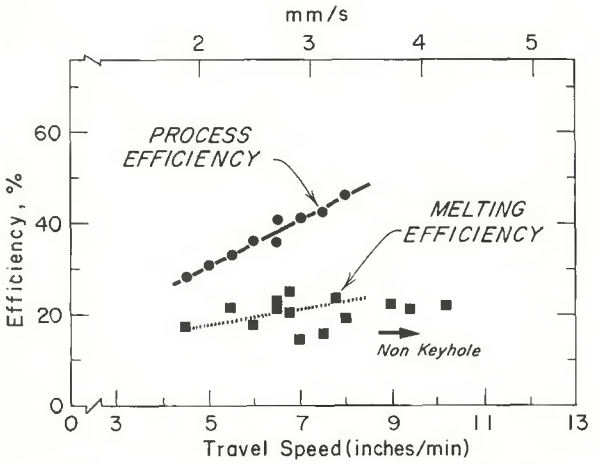

Fig. 8 — Effect of travel speed on process and melting efficiency

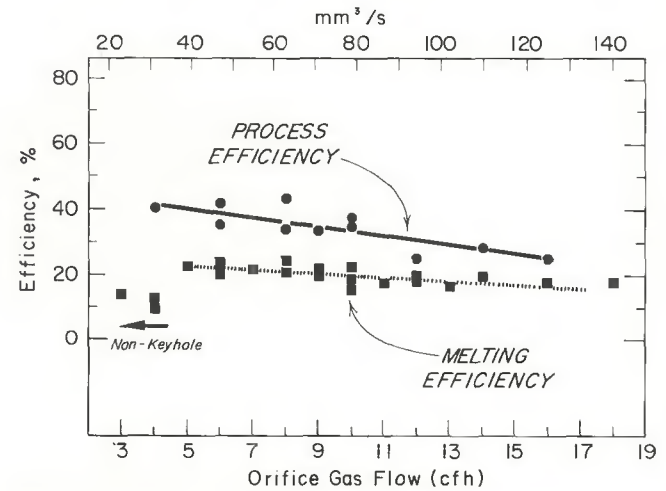

Fig. 9 — Effect of orifice gas flow rate on melting and process efficiency

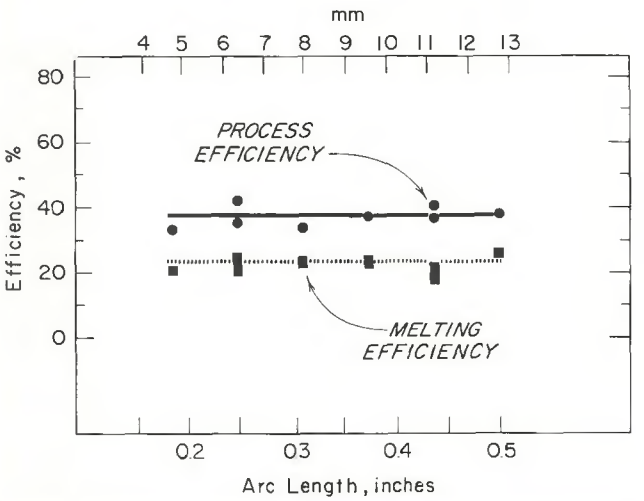

Fig. 10 — Effect of arc length on melting and process efficiency

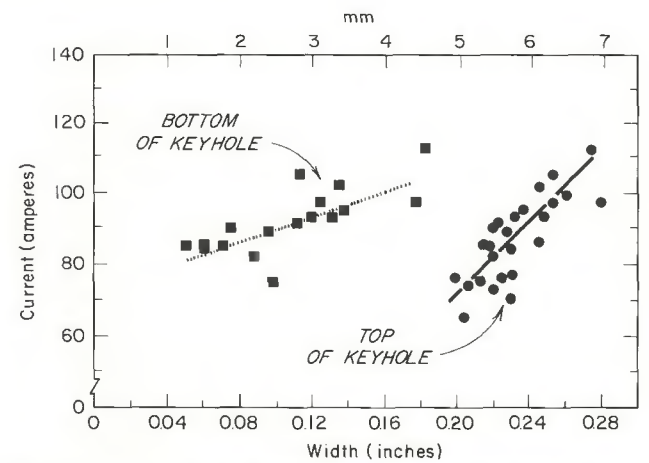

Fig. 11 — Relationship between current and the top and bottom widths of keyhole mode plasma arc welds

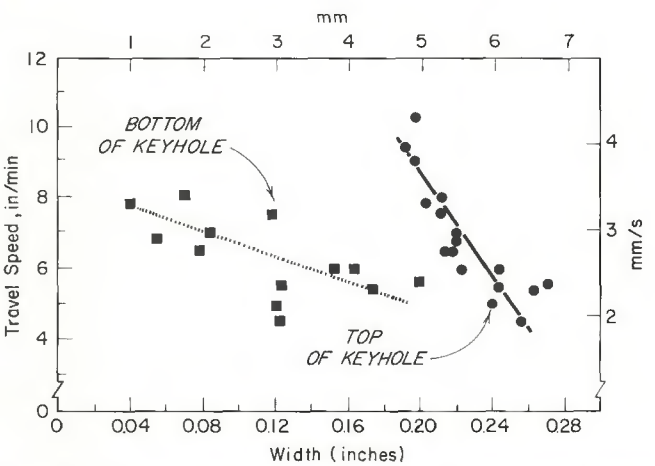

Fig. 12 — Relationship between travel speed and the top and bottom widths of mode plasma arc welds

a larger percentage of the heat to go out the bottom of the weld.

The arc length was varied keeping the heat input and orifice gas flow constant, and the process and melting efficiency was plotted against arc length, as shown in Fig. 10. As the arc length increases, the process and melting efficiency show little change. As the arc length increases, the keyhole bottom width becomes smaller so that the heat loss out the bottom decreases, and the effect of the orifice gas flow diminishes.

Top and Bottom Keyhole Width

When making a keyhole mode weld, the application is usually to a butt joint on thin material or the root pass for thicker material. One of the purposes of keyhole mode plasma welding is full penetration with good back side appearance. If the joint fitup is extremely good, a very small bottom size keyhole width is necessary. If the joint fitup is poor, a wider bottom width helps compensate for the poor fitup. Figures 11 and 12 show how the top and bottom width is affected by parameter changes such as current and travel speed. As the heat input increases either by increasing the current or decreasing the travel, the top and the bottom width of the keyhole increases. It is also to be noted that the bottom width increases at a faster rate than the top width.

Considering the data available, if a wider bottom keyhole size is desired, three possible directions can be taken, each with its own limitations.

1. If the heat input is increased not only will the bottom width increase, but the top width will also increase. Increasing the heat input will slow down the cooling rate which may produce a detrimental structure in the heat-affected zone of the weld, also increasing the heat input may increase the weld puddle to a size where a keyhole cannot be maintained.

2. If the arc length is decreased, the bottom width will become greater and the top width smaller, which is beneficial from a depth to width ratio standpoint; however, there is a physical limit to how close the water cooled orifice can be placed to the weld puddle without rapid eroding of the orifice.

3. Increasing the orifice flow rate will widen the bottom of the keyhole without appreciably affecting the top width of the keyhole. However, the greater the orifice flow rate, the greater the drop through on the bottom side and the more undercut that is present on the top side. This undercut can be improved by the addition of hot or cold filler metal. Filler metal addition can also supply the extra weld metal needed when poor fitup occurs.

The next step was to determine how the energy across the plasma-

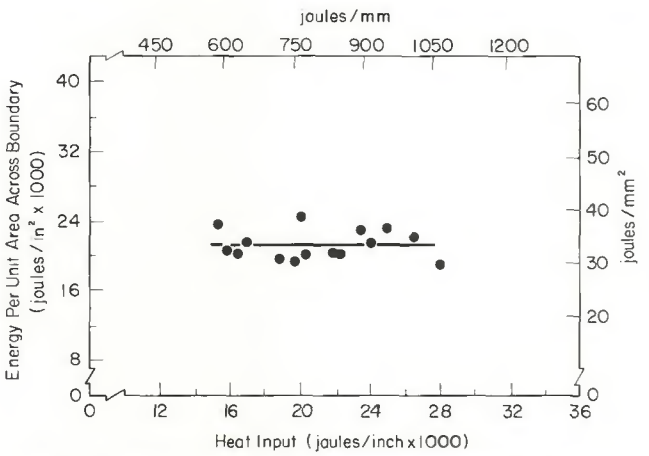

Fig. 13 — Relationship between energy per unit area across the plasma molten metal boundary and the heat input for keyhole mode plasma arc welds

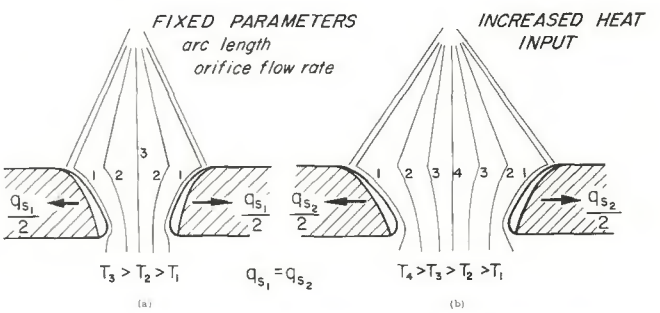

Fig. 14 — Shows two keyhole mode plasma arc welds with all the welding parameters held constant except heat input; (b) has an increased heat input over (a)

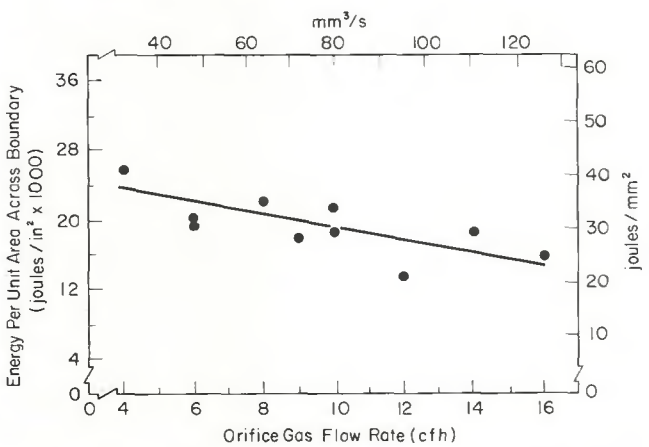

Fig. 15 — Relationship between the energy per unit area across the plasma molten metal boundary and the orifice gas flow rate for keyhole mode plasma arc welds

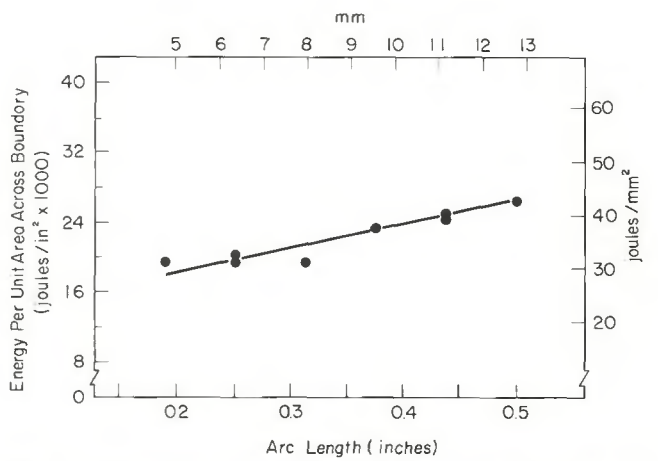

Fig. 16 — Relationship between the energy per unit area across the plasma molten boundary and the arc length for keyhole mode plasma arc welds

liquid metal boundary varies with the welding parameters. Figure 13 shows the effect of heat input on the energy per unit area, q_s, for welds where the arc length and orifice gas flow was kept constant. As the heat input changes, the energy per unit area remains fairly constant. This implies that as the shape and temperature distribution of the arc changes, the energy per unit area transferred from the arc to the molten metal remains constant. This further implies that the temperature of the arc plasma at the molten metal boundary remains constant as the heat input changes. This can be better understood from Fig. 14. The contact length over the range of heat inputs remains fairly constant, so the keyhole boundary seeks an equilibrium condition which permits the energy per unit area to remain constant.

The relation of the energy per unit area, q_s, to the orifice flow rate for the welds is shown in Fig. 15. The energy per unit area decreases when the orifice flow rate increases. This implies that when the orifice flow rate increases, the plasma boundary temperature decreases. As the orifice flow rate increases, the top width of the keyhole remains fairly constant. This implies that the outer edges of the arc shape at the top of the weld do not change much with the flow rate. Since the energy to the arc was constant for these weld samples, the arc energy is forced deeper into the weld due to the increased force of the plasma. As a consequence, the bottom of the keyhole becomes wider as the orifice flow rate is increased.

The third step was to plot the energy per unit area, q_s, versus changes in arc length, with the current, travel speed, and orifice gas flow rate kept constant. Figure 16 indicates that as the arc length increases, the energy per unit area increases. When the arc length increases, the effect of the arc on the base metal decreases which gives the same effect as decreasing the orifice gas flow. Decreasing the orifice gas flow increases the energy per unit area as shown previously. Therefore, increasing the arc length changes the energy per unit area at the plasma-molten metal boundary and has the same effect as decreasing the orifice flow rate.

The welding parameters can be used to change the shape of the keyhole to accommodate for changes in joint design and fitup. In welding one pass keyhole welds, a major concern is that no detrimental structures are produced in the heat-affected zone of the weld. The base metal structures in the heat-affected zone are produced by the peak temperatures and the time at temperature that are obtained. The energy per unit area across the molten plasma boundary determines the peak temperature that is reached at a certain point in the heat-affected zone. The energy per unit area or peak temperature is not affected by the heat input but only by the orifice flow rate and arc length. However, the heat input does influence the cooling rate or time-temperature relations. The greater the heat input the slower the cooling rate. For the best properties in the heat-affected zone, low peak temperatures and fast cooling rates are desired. This condition would be optimized by short arc lengths, high orifice flow rates and low heat input. However, these conditions cannot always be optimized due to considerations of bead appearance and bead shape.

Conclusions

The following are the conclusions derived from the results of this investigation of plasma arc welds in ⅛ in. (3 mm) thick 304 stainless steel.

1. Process efficiency, melting efficiency, and the percent of energy transferred to the heat-affected zone:
   a. decrease as the current is increased
   b. increase as the travel speed is increased
   c. decrease as the orifice gas flow rate is increased
2. The top width of the keyhole weld:
   a. increases as the current is increased
   b. decreases as the travel speed is increased
   c. remains constant as the orifice gas flow rate is increased
   d. increases as the arc length is increased
3. The bottom width of the keyhole weld:
   a. increases at a faster rate than the top width as the current is increased
   b. decreases at a faster rate than the top width as the travel speed is increased
   c. increases as the orifice flow rate is increased
   d. decreases as the arc length is increased
4. The energy per unit area across the plasma-molten liquid boundary:
   a. remains constant over the range of heat inputs that were used
   b. decreases as the orifice flow rate is increased
   c. increases as the arc length is increased

Acknowledgement

The authors wish to express their appreciation for the support provided by the Union Carbide Corporation, Linde Division. Their financial support provided the Fellowship fund and donations of equipment made the program possible. Stainless steel plate for the tests was donated by Williams and Co., Inc. Technical and material assistance from others is also acknowledged.

References

1. Gross, B., Gavcz, B. and Mikossy, K., *Plasma Technology,* American Elsevier Publishing Company, Inc., New York, 1969, pp. 248-250.

2. Ludwig, H. C., "Plasma-Energy Transfer in Gas-Shield Welding Arcs", *Welding Journal,* Vol. 38, (7), July 1959, Res. Suppl., pp. 296s-300s.

3. Eckert, E. R. G. and Pfender, E., "Plasma Energy Transfer to a Surface With and Without Electric Current", *Welding Journal,* Vol. 46 (10), October 1967, Res. Suppl., pp. 471s-479s.

4. "Progress in Plasma Technology", *Welding and Metal Fabrication,* February 1970, pp. 46-50.

5. Wilson, E. M., "Micro-Plasma Arc Welding of Thin High Strength Steel Strip", *Welding and Metal Fabrication,* April 1968, pp. 133-138.

6. Gage, R. M., "The Principles of the Modern Arc Torch", *Welding Journal,* Vol. 38, (10), October 1959, pp. 959-962.

7. "Plasma Arc Welding", *Welding and Metal Fabrication,* May 1966, pp. 162-170.

8. O'Brien, R. L., "Arc Plasma for Joining, Cutting and Surfacing", *Welding Research Council Bulletin,* 131/July 1968.

9. Cooper, G., Palermo, J., Browning, J. A., "Recent Development in Plasma Welding", *Welding Journal,* Vol. 44, (4), April 1965, pp. 268-276.

10. Arata, Yoshiaki and Maruo, Hiroshi, "Magnetic Control of Plasma Arc and Its Application for Welding", International Institute of Welding Doc. IV-53-71, March 1971.

11. Bratkovich, Nick F., "Plasma Arc Welding", 1970, American Society for Metals, Conference on Modern Joining Techniques.

12. Okada, Minoru; Maruo, Hiroshi, Namba, Keizo, "Studies on Plasma Welding", Technology Reports of the Osaka University, Vol. 17, No. 752.

13. Hasui, Atsushi, Kasahara, Eiji, Taguchi, Hiroya, "Studies on Plasma Arc Welds", Transactions of the National Research Institute for Metals, Vol. 10, No. 6 (1968).

14. Rosenthal, D., "Mathematical Theory of Heat Distribution During Welding and Cutting", *Welding Journal,* Vol. 20, (5), May 1941, Res. Suppl., pp. 223-234.

15. *Physical Constants of Some Commercial Steels at Elevated Temperatures,* London Butterworks Scientific Publications, 1957.

16. Wicks, C. E., Block, F. E., *Thermodynamic Properties of 65 Elements — Their Oxides, Halides, Carbides, and Nitrides,* Bulletin 605, Bureau of Mines, United States Government Printing Office, Washington, D.C., 1963.

17. Christensen, N., Davies, L., and Gjermundsen, K., "Distribution of Temperatures in Arc Welding", *British Welding Journal,* February 1965, pp. 54-75.

18. Niles, Wayne, R., *An Examination of Weld Thermal Efficiency,* Master's Thesis, The Ohio State University, 1969.

AWS PUBLICATIONS ON BRAZING

A5.8-69 Specification for Brazing Filler Metal

This filler metal spec covers the requirements for filler metals which are added when making a braze. Superseding the 1960 edition, the current version states labeling requirements for brazing filler metals and establishes required mesh sizes for powdered filler metals.

Brazing Manual

The brazing materials used in aerospace, nuclear, and electronic industries, the brazing of electron tubes and vacuum equipment, and honeycomb-structure brazing are just some of the topics spotlighted in the BRAZING MANUAL. The text also covers the commonly brazed base metals such as aluminum, stainless steels, and nickel alloys, and includes discussions of joint design, brazing equipment and techniques, fluxes and atmospheres, and the inspection of brazed joints. A chapter is devoted to the ASME Boiler Code brazing provisions.

C3.2-63 Standard Method for Evaluating the Strength of Brazed Joints

The brazing industry has never had a standardized test specimen that is to brazements what the 0.505 inch tensile bar is to weldments. This publication provides a common basis for comparing filler metals and brazing procedures among different organizations.

Braze Safely

"Braze Safely" is an illustrated, eight-panel brochure describing the "Do's and "Don't" of proper brazing when using cadmium-bearing silver filler metals. Aimed primarily at brazers and shop supervisors, the brochure tells how to prevent generation of hazardous cadmium and fluoride fumes by implementing safe brazing techniques. Presented in a convenient, easily readable format, "Braze Safely" is an excellent guide for all shop personnel involved in brazing.

Prices*

A5.8—69 Specification for Brazing Filler Metal	$2.00
Brazing Manual	$7.50
C3.2-63 Standard Method for Evaluating the Strength of Brazed Joints	$1.00
Braze Safely (minimum order: 100 copies)	$5.00 per 100

**Discounts: 25% to A and B members; 20% to bookstores, public libraries and schools; 5% to C and D members. Add 4% sales tax in Florida.*

Send your orders for copies to the American Welding Society, 2501 N. W. 7th Street, Miami, Florida 33125.